

Transverse and in-plane modification of superconductivity and electronic structure in the quasi-two dimensional organic conductor κ -(BEDT-TTF)₂Cu(SCN)₂ by uniaxial stress

E. S. Choi^{a,b} J. S. Brooks^a S. Y. Han^a L. Balicas^{a,c}
J. S. Qualls^a

^a*National High Magnetic Field Laboratory and Florida State University,
Tallahassee, FL 32310, USA*

^b*Research Institute for Basic Sciences, Seoul National University, Seoul 151-742,
Korea*

^c*Instituto Venezolano de Investigaciones Científicas, Apartado 21827, Caracas
1020A, Venezuela*

Abstract

We have employed uniaxial stress along the principal axes of the quasi-two dimensional organic superconductor κ -(BEDT-TTF)₂Cu(SCN)₂. The lattice anisotropy is thereby altered, with corresponding changes in the intermolecular transfer energies. The effect of uniaxial stress on the superconducting transition temperature T_c and critical field B_{c2} is found to be anisotropic. There is an indication of an increase in T_c and B_{c2} for in-plane stress, but both parameters decrease rapidly for transverse (inter-plane) stress. Magnetotransport studies reveal stress-induced changes in the Fermi surface through the observation of the Shubnikov de Haas oscillations. The stress dependence of a resistive anomaly in the magnetoresistance, which is associated with the critical field B_{c2} , is also investigated. We discuss the experimental findings in the context of recent phenomenological and theoretical treatments of quasi-two dimensional systems where the anisotropic triangular lattice Hubbard model has been used to treat two-dimensional superconductors.

Key words: A. Organic crystal; A. Superconductors; D. Electronic transport; E. High pressure

1 Introduction

The quasi-two-dimensional organic superconductor families, κ -(BEDT-TTF)₂X (X = Cu(NCS)₂, Cu[N(CN)₂]Br, Cu[N(CN)₂]Cl), have been widely studied both experimentally and theoretically [1]. Depending on the species of the anion (X) and the pressure, these compounds can exhibit ferromagnetic, antiferromagnetic, insulating, or superconducting ground states. These "kappa-phase" materials have been the subject of considerable recent attention due to reports of evidence for d-wave superconductivity[2][3], [4],[5], as well as reports to the contrary [6]. Fig. 1 shows the molecular stacking and the Fermi surface of κ -(BEDT-TTF)₂Cu(SCN)₂, which is the subject of this report. This material is a superconductor with a transition temperature $T_c = 10.4$ K. Theoretically, the anisotropic triangular lattice Hubbard model has been used to treat the kappa-phase ground states[7–12]. In the triangular lattice model, each BEDT-TTF dimer is treated as a single lattice point in the triangular lattice with four nearest neighbors with transfer integral t_2 and two next nearest neighbors with transfer integral t_1 (See Fig. 1a). Hence the system is modeled as a triangular arrangement with one electron on each vertex site. For favorable ratios of t_1 and t_2 , unconventional pairing (superconductivity) may arise from antiferromagnetic fluctuations, with the interaction modeled by the on-site Coulomb repulsion U . The consensus of these models is that the most likely superconducting order parameter symmetry is d-wave. Furthermore, Kondo and Moriya have predicted[9,12] a maximum in T_c for particular values of t_1 and t_2 (see Discussion section).

The motivation for the present work has been, therefore, to apply in-plane uniaxial stress in order to modify t_1 and t_2 , and to monitor corresponding changes in the transition temperature, and other physical properties in a κ -phase superconductor with high magnetic fields. The most important results are:

- 1) the very weak dependence of T_c and B_{c2} on in-plane stress, which in some cases actually increase;
- 2) the stress-dependent nature of the resistive anomaly in the magnetoresistance which has been ascribed to unconventional superconductivity;
- 3) through the observation of the Shubnikov de Haas oscillations, we describe changes in the Fermi surface with stress, and indirectly, changes in the lattice constants.

For completeness, in Tables I and II we present a summary of previous and present results which treat T_c and corresponding changes in the Fermi surface topology of κ -(BEDT-TTF)₂Cu(SCN)₂ salt under hydrostatic pressure, tensile stress, thermal expansion, and uniaxial stress.

2 Experiment

κ -(BEDT-TTF)₂Cu(SCN)₂ single crystals were grown by conventional electrochemical crystallization. Typical dimensions of the samples were (for $a \times b \times c$) $0.1 \times 0.6 \times 0.9 \text{ mm}^3$ with the b - c plane corresponding to the most conducting plane. Uniaxial stress was applied by using the epoxy encapsulation method [13]. Polarized infrared (IR) reflectance in the range of $650 - 3500 \text{ cm}^{-1}$ was employed to determine the b - and c -axis orientations [14]. Samples were cut into two or three pieces to use for the three orientations, a -, b -, or c -axis, and electrical contacts were made with $12.5 \text{ }\mu\text{m}$ gold wires attached with silver paste. A conventional 4-terminal AC technique was used with a frequency of $\sim 17 \text{ Hz}$, and an ac current of $10 \text{ }\mu\text{A}$ was applied along the least conducting axis (a -axis). The magnetic field was applied along the a -axis, perpendicular to the conducting b - c plane. For magnetoresistance measurements where stress in the b - c plane was studied, a novel device was used to transmit stress along the in-plane direction with the applied magnetic field perpendicular to the direction of stress [15]. In all cases, stress was applied in situ, at low temperatures, in increasing increments.

3 Results

3.1 Uniaxial stress dependence of T_c

Fig. 2 shows the change of the superconducting transition T_c of κ -(BEDT-TTF)₂Cu(SCN)₂ for uniaxial stress along the in-plane, c -axis direction. The value of T_c obtained from the ambient pressure (no epoxy) measurements is almost identical to that of the samples with epoxy (at zero pressure), but some of the samples showed a wider transition width and/or finite residual resistance below T_c . In this work we define T_c from the maximum in the resistance-temperature derivative (dR/dT) in the range of the transition, as shown in the inset of Fig. 2. Hence over the range of 8 kbar, T_c decreases only by about 20%, but the normal state resistance decreases by a factor of six.

A summary of the uniaxial stress experiments along the a -, b - c -, and c - axes is shown for 1 bar, 2.5 kbar, and 5 kbar in Fig. 3. Also shown is the case where stress was applied along an arbitrary $b - c$ in-plane direction. The changes in T_c for all four experiments are shown in Fig. 4, and values of $\partial T_c / \partial P_{a,b,c}$ from the present work are given in Table 1, which, by inspection, shows that the changes in T_c are substantially less (and/or non-monotonic) for in-plane stress, when compared with either a -axis stress or hydrostatic pressure.

3.2 Uniaxial stress dependence of the magnetoresistance at 0.5 K

3.2.1 Magnetoresistance for a-axis stress

Further differences between inter-plane and in-plane stress on the superconducting properties can be seen with magnetic field. In Fig. 5 we present the magnetoresistance (MR) for κ -(BEDT-TTF)₂Cu(SCN)₂ at 0.5 K for stress applied along the a-axis. (Similar measurements for *a*-axis stress, which is along the inter-plane direction, have been previously reported [16], but have been re-measured in this work for completeness). The data, which are offset for clarity, show several distinct trends with increasing stress: the quantum oscillation spectrum changes, the critical field B_{c2} decreases, and the normal state resistance also decreases. The Fourier spectrum for a-axis stress is shown in Fig. 6a. The fundamental orbit α and its harmonic 2α rapidly attenuate with stress, but the magnetic breakdown orbit β and its combination frequencies $\beta \pm \alpha$ present a more complicated stress dependence (see Fig. 1b). At 2 kbar and above, the magnetic breakdown orbit β is dominant, and α only appears in the $\beta + \alpha$ spectrum. In Fig. 6 b and 6c we show the a-axis stress dependence of the Fourier spectrum. The main result of Fig. 6 is that the β orbit, which is proportional to the area of the first Brillouin zone (and inversely proportional to the in-plane unit cell), decreases with increasing a-axis stress. That the fundamental α increases has been previously discussed by Campos et al.[16]. Although it is not possible to predict in detail, it is clear that the symmetry of the Fermi surface, and therefore the underlying unit cell, has been changed in some non-trivial manner. In Fig. 7 we show the decrease in the critical field with a-axis stress, as determined from the maximum in the derivative dR/dB (see inset of Fig. 7).

3.2.2 Magnetoresistance for b-axis stress

We selected the *b*-axis configuration for high field studies with in-plane stress since a change of lattice constant in this direction would allow t_1 to increase with respect to t_2 , i.e. make the triangular lattice model more "equilateral". Also, the *b*-axis strain showed the least decrease in T_c of the three principal axes (Fig. 4). The MR data for b-axis stress are shown in Fig. 8 at 0.5 K. Unlike the a-axis results in Figs. 5-7, the b-axis have a different Fourier SdH spectrum dependence on stress, and the critical field B_{c2} appears to increase with stress. In Fig. 9a the Fourier spectrum shows that the magnetic breakdown β orbit amplitude more rapidly attenuates with stress than does the α orbit amplitude. Also, the changes in frequency are very small. To see them clearly, we show a single SdH period in Fig. 9b, where a particular Landau level is observed to move to lower fields with stress. This corresponds to a decrease in the α orbit frequency, as shown in Fig. 9c. In Fig. 10 we show

the behavior of the critical field B_{c2} as defined from dR/dB (see inset of Fig. 10). The fact that B_{c2} increases is the most dramatic effect of the in-plane stress in the magnetoresistance.

3.3 Uniaxial stress dependence of the magnetoresistance anomaly

At higher temperatures, the critical field signature becomes complicated by a magnetoresistance anomaly (defined as ΔR in Fig. 11) which appears in this materials, and which disappears for in-plane magnetic field [17]. The higher temperature behavior of this anomaly, which is a peak in the MR just above B_{c2} , is shown for both stress directions in Fig. 11. For the a-axis case, with increasing stress, the peak rapidly attenuates, and B_{c2} decreases. For increasing b-axis stress, the peak decreases, but B_{c2} increases, as it did at 0.5 K (see Fig. 10) for the highest stress values. In Fig. 12 we show the full temperature and stress dependence of the anomaly from our measurements as a function of $\Delta R/R_N$, where R_N is defined as the normal state resistance extrapolated from fields higher than B_{c2} (see Fig. 11b).

3.4 Analysis of normal state properties

Further information may be obtained from the normal state properties. From the temperature dependence of the SdH oscillation amplitudes the effective masses $m^* = m_{SdH}/m_0$ of the carriers in the various orbits may be obtained, either from the wave forms directly, or from the amplitudes of the Fourier spectrum[18]. A summary of our findings is shown in Fig. 13 for the high magnetic field data. For the a-axis data, the SdH effect could not be observed above 2.5 kbar, although there is some evidence that m^* is decreasing for the α and β orbits. Campos et al. also found that for a-axis stress, the SdH effect vanished at low values (of order 2 kbar), along with T_c and B_{c2} . In the case of the b-axis, we could follow the SdH effect for the α orbit over the entire range of stress. Within the uncertainties of the determination, there is very little change in m^* . In Figure 14 we present the stress dependent normal state resistance change for $a-$, $b-$, and $c-$ axis stress. The apparent difference in functional dependence between inter-plane and in-plane stress is represented by the two different fits (solid lines), as discussed in the next section.

4 Discussion

4.1 Uniaxial stress effects on crystallographic and electronic structure

In order to gauge the effects of uniaxial stress on the crystallographic structure, we consider the a-axis stress dependence of the β orbit, as shown in Fig. 6 and Table 2. The frequency of the F_β orbit is directly related to the total area of the first Brillouin zone, $A_{BZ} = 2\pi/b * 2\pi/c$. For small changes, $\Delta F_\beta/F_\beta \approx \Delta A_{BZ}/A_{BZ} \approx -\Delta(bc)/bc$. Hence the stress dependence of β is directly related to the in-plane lattice parameters. We may therefore estimate an approximate linear compressibility by considering the constant volume deformation of a system with isotropic elasticity. For a cubic lattice of side a , the fractional reduction in lattice constant (per kbar) along one axis is $\epsilon = \delta a/a$ (kbar^{-1}). This will produce an expansion (i.e. Poisson effect) of $\epsilon/2$ in the orthogonal directions. Hence, using the cubic lattice-isotropic compressibility approximation, $\Delta F_\beta/F_\beta \approx 2\delta a/a$, and from Table 2, $\epsilon = -0.0035/\text{kbar}$ for the a-axis compressibility of κ -(BEDT-TTF)₂Cu(SCN)₂.

From simple ‘‘Golden rule’’ arguments, the conductivity due to any single direction in the tight binding limit should increase as t^2 . Hence, for an approximately linear response of t to uniaxial stress along the a-axis, the a-axis conductivity change would be $\sigma \approx \sigma_0(1 - 2\epsilon P_a)$. The resistivity will therefore decrease inversely as $R(p)/R(0) = (1 - 2\epsilon P_a)^{-1}$ with pressure. For the cases where both the a-axis resistivity and stress are involved, this relation seems to represent the data, with the caveat that the in-plane changes in conductivity have been neglected. In reference to Fig. 14, we find for the two a-axis cases studied, that $\epsilon = 0.17 \pm 0.1/\text{kbar}$. The larger, fitted value of ϵ (compared with the estimate above) from the normal state resistance may reflect a stronger dependence of t on ϵ than the linear approximation used in the argument above. In contrast, the in-plane stress yields a very different pressure dependence for the a-axis conductivity. Here, the decrease of the normal state resistance can be fitted empirically by $R(p)/R(0) = 1 - (p/p_c)^2$, where p_c is 10.7 ± 0.1 kbar. This strongly suggests that the effects of b-axis in-plane stress on the transverse conductivity involve competing effects.

We next turn to stress induced changes in the Fermi surface properties, which may be obtained by considering the SdH oscillations. Returning to Fig. 6, we see two different frequencies, $F_\alpha \approx 670T$ and $F_\beta \approx 4200T$. A summary of changes in F_α and F_β for both uniaxial and hydrostatic pressure is given in Table 2. In reference to Fig. 1b, F_α arises from the closed orbit and F_β is a magnetic breakdown orbit which involves both the closed and open orbit Fermi surface sections. The amplitude of F_β depends on the proximity of the closed and open orbit Fermi surface sections, since a magnetic breakdown gap is involved in the orbit. For the case of a-axis stress in Fig. 6, the shift of relative amplitude from the α to β Fourier spectrum may indicate the closing of the magnetic breakdown gap. Although the β orbit decreases as

expected for the expansion of the real space b-c plane with a-axis stress, the α orbit increases significantly. A model for the sliding of the (BEDT-TTF) molecules has been proposed to explain this effect[16,19]. In contrast, changes in the electronic structure for b-axis stress are very much reduced. Changes in F_α and F_β are very small, and the α orbit is always dominant - hence the magnetic breakdown gap remains large. Since, for a reduction of the b-axis lattice constant, the c-axis lattice constant should increase by the Poisson argument, this may explain why F_β does not change significantly. Although small, the b-axis change in F_α is opposite that for a-axis stress, and this indicates that stress in the two directions produce fundamental differences in the changes of electronic structure.

A treatment of the temperature dependence of the SdH amplitudes in terms of the Lifshitz-Kosevich analysis[18] yields information about the effective mass m^* ($= m/m_e$), which can be enhanced by many body effects (electrons and phonons). We have summarized our analysis of m^* for a-axis and b-axis stress in Fig. 13., where the effective masses of the α and β orbits (m_α and m_β) are shown as a function of stress. m_α appears to be nearly stress-independent for both axes, while m_β begins to decrease for $P > 2$ kbar.

4.2 Uniaxial stress effects on superconductivity

In this final section we review the effects of uniaxial stress on the superconducting state in relation to the observed changes in the electronic structure, and comment on our results in the context of recent theoretical work. One of the original motivating factors in this work was to use in-plane stress to change the ratio of t_1/t_2 as shown in Fig. 1a. Following arguments similar to those of the last section (for a cube of constant volume and isotropic elasticity), the application of stress along the b-axis will produce changes in t_1/t_2 of order $(1 - \epsilon P_b)/(1 + \epsilon P_b/4)$, or for 10 kbar, about +4%. (We note however, that since changes in t are approximated as linear in ϵ , the relative change in t_1/t_2 may be significantly larger, as the fit of ϵ in Fig. 14 indicates.) For a-axis stress, a simple Poisson-like uniform expansion of the in-plane lattice should not, to first order, cause the ratio t_1/t_2 to change.

For comparison, Kondo and Moriya have used a two band Hubbard model with spin fluctuations[9,12] to compute the dependence of T_c on U/t_2 and t_1/t_2 . Referring to Fig. 2 of Ref. [12]), these parameters are: $t_1 \approx 0.07eV$; $t_2 \approx 0.0875eV$; and $U \approx 0.75eV$. They predicted, using a d-wave symmetry for the order parameter, that for fixed t_1/t_2 in the range 0.4 to 0.8, T_c/t_2 versus U/t_2 would show a maximum change of between +50% and +10% for intermediate values of $(U/t_2)^*$ in the range 4 to 10. Vojta and Dagotto also have considered the triangular lattice problem[11] and find a tendency for d-

wave paring for $t_1/t_2 \leq 0.8$. Clearly, we cannot determine from our in-plane results accurate experimental changes in t_1/t_2 and U/t_2 , primarily due to the large uncertainties in our estimates of ϵ . Nevertheless our in-plane data suggest that T_c , as well as the critical field B_{c2} , follow a significantly different dependence on in-plane stress, when compared either with inter-plane stress, or with hydrostatic pressure.

A second area of comparison with theory involves the magnetic breakdown gap. Schmalian has used a two band Hubbard model with spin fluctuations[20] to predict d-wave superconductivity for the κ -phase materials for the Fermi surface described in Fig. 1. A key feature of this theory is the inter-band coupling, which is influenced by the magnetic breakdown gap region ("hot spots" in the terminology of Ref. [20]). Experimentally, we see that for a -axis stress this magnetic breakdown gap appears to be closing, and correspondingly, the superconducting transition and critical field decrease. Following Fig. 3 of Ref. [20], if the gaps closed, then the additional nodes along the diagonals of the d-wave gap symmetry would disappear, but this would not destroy the d-wave state. Conversely, for b -axis stress we note that the magnetic breakdown gap does not close, the superconducting transition is only a weak function of stress, and the critical field actually increases.

A third point concerns the resistive anomaly which occurs in the critical field behavior at temperatures of larger than 25 % of T_c , as shown in Figs. 11 and 12. This anomaly seems to be a common feature of low dimensional, layered superconductors, including high- T_c cuprates and non-Cu based organic superconductor [21,22]. The effect is quite anisotropic, and is found to be most significant when the current and the field are applied perpendicular to the conducting plane[17]. The reduction of ΔR with stress can be quantitatively described by plotting $\Delta R/R_N$ versus stress as shown in Fig. 12, where ΔR is the difference of resistance at $B = B_{\max}$ and R_N is the normal state resistance obtained from the extrapolation from $B \gg B_{c2}$ (See Fig. 11). $\Delta R/R_N$ is largest at higher temperatures, and decreases with stress for fixed temperature. This extra resistance has been attributed to various mechanisms. One involves the presence of magnetic impurities [23], but since the impurity concentration would not change with stress, the present work is inconsistent with a magnetic impurity effect. There are several other models which treat this effect in terms of interplaner coupling effects. One involves the inter-layer resistance due to Josephson junction coupling[22]. A second model is that of Maki and co-workers[24]. Here the anomaly is treated as a superconducting fluctuation mechanism, with the conclusion that the interplane magnetoresistance can only arise from d-wave symmetry. Finally, Kartsovnik and co-workers[25] conclude that the interlayer transport in the superconducting state is mediated by superconducting-normal-superconducting Josephson tunneling. Both models support the highly anisotropic nature of the anomaly in tilted fields. Since ΔR is most sensitive to the a -axis interplaner stress, interplaner coupling

effects may indeed be the origin of this effect.

Finally, we note dependence of the effective masses on uniaxial stress shown in Fig. 13. If we assume the change of T_c follows the weak-coupling BCS scheme, T_c is a strong function of effective mass m^* . This trend does appear to some extent in the a-axis data, with both m^* (over the small range measured) and T_c decreasing. For the b-axis data, the weak dependence of m^* and T_c on stress appears to be mutually consistent.

5 Conclusions

In summary, we have employed both inter-planar (transverse) and in-plane uniaxial stress to physically change parameters associated with the triangular lattice model for superconductivity in the quasi-two dimensional metal κ -(BEDT-TTF)₂Cu(SCN)₂. Our main results show that the superconductivity associated with inter-planar stress is rapidly reduced, as is observed in the critical temperature, the critical field, and also in the resistive anomaly associated with the critical field. The normal state resistance follows a simple model for the increase of inter-planar band-width with stress. For in-plane stress, a more direct modification of the parameters of the triangular lattice model is possible. Indeed, for in-plane stress, the critical temperature is a considerably weaker function of stress, and may even increase slightly over a small range. Also, the critical field is observed to increase significantly, and the resistive anomaly associated with the critical field is not a strong function of in-plane stress. Here the normal state resistance is a more complicated function of in-plane stress. We have used the SdH effect to monitor stress-induced changes in the unit cell and electronic structure. The most dramatic changes occur for the a-axis case where the fundamental closed orbit area increases by 10%, and the inter-band magnetic breakdown gap essentially disappears. In contrast, the in-plane stress does not significantly change the SdH parameters associated with the Fermi surface, except that the fundamental closed orbit decreases with b-axis stress. Also, the magnetic breakdown gap remains open.

We find provocative, but inconclusive comparisons with contemporary theories for d-wave superconductivity in this "kappa phase" material. Over the the range of parameters investigated, there is no single aspect of the electronic structure to which the superconductivity is highly sensitive, but we emphasize that the in-plane modification of the lattice parameters has the most unusual effects on the superconducting state. Application of strictly uniaxial stress via methods now employed by several groups [26] [27], coupled by higher values of stress, perhaps to 20 kbar, should allow the ratio t_1/t_2 to change enough to more fully test the predictions of the triangular lattice Hubbard models.

Acknowledgements This work was supported in part by NSF-DMR95-10427 and DMR99-71474. The work was carried out at the National High Magnetic Field Laboratory, supported by a contractual agreement between the State of Florida and the NSF through NSF-DMR-95-27035.

References

- [1] T. Ishiguro, K. Yamaji, *Organic Superconductors*, Springer-Verlag, Berlin, 1990.
- [2] J. M. Schrama, E. Rzepniewski, R. S. Edwards, J. Singleton, A. Ardavan, M. Kurmoo, and P. Day, *Phys. Rev. Lett.* **83**, 3041 (1999).
- [3] Y. Nakazawa and K. Kanoda, *Phys. Rev. B* **55**, R8670 (1997).
- [4] A. Carrington, I. J. Bonalde, R. Prozorov, R. Giannetta, A. M. Kini, J. Schlueter, H.H. Wang, U. Geiser, and J. M. Williams, *Phys. Rev. Lett.* **83**, 4172 (1999)
- [5] M. Pinteric, S. Tomic, M. Prester, D. Drobac, O. Milat, K. Maki, D. Schweitzer, I. Heinen, W. Strunz, *Phys. Rev. B* **61**, 7033(2000)
- [6] H. Elsinger, J. Wosnitza, S. Wanka, J. Hagel, D. Schweitzer, and W. Strunz, *Phys. Rev. Lett.* **84**, 6098(2000).
- [7] H. Kino and H. Fukuyama, *J. Phys. Soc. Jpn.* **65** (1996) 2158.
- [8] H. Kino and H. Kontani, *J. Phys. Soc. Jpn.* **67** (1998) 3691.
- [9] H. Kondo and T. Moriya, *J. Phys. Soc. Jpn.* **67** (1998) 3695.
- [10] R. H. McKenzie, *cond-mat/98021198*. Also appear in *Comments Cond. Matt. Phys.* **18** (1998) 309.
- [11] M. Vojta and E. Dagotto, *Phys. Rev. B* **59** (1999) R713.
- [12] H. Kondo and T. Moriya, *cond-mat/9903374*.
- [13] C. E. Campos, J. S. Brooks, P. J. M. van Bentum, J. A. A. J. Perenboom, J. Rook., S. J. Klepper, M. Tokumoto, *Rev. Sci. Inst.* **66** (1995) 1061. By adding Si-C microfiber into the epoxy, uniaxial stress to 8 kbar can be reliably achieved.
- [14] A. Ugawa, G. Ojima, K. Yakushi and H. Kuroda, *Phys. Rev. B* **38** (1988) 5122.
- [15] J. S. Brooks, J. S. Qualls, C. E. Campos and J. A. A. J. Perenboom, *Synth. Met.* to be published.
- [16] C. E. Campos, J. S. Brooks, P. J. M. v Bentum, J. A. A. J. Perenboom, S. J. Klepper, P. Sandhu, M. Tokumoto, T. Kinoshita, N. Kinoshita, Y. Tanaka and H. Anzai, *Physica B* **211** (1995) 293.

- [17] F. Zuo, J.S. Brooks, R. H. McKenzie, J.A. Schlueter, J.M. Williams, *Phys. Rev. B* **61**, 750(2000).
- [18] J. Wosnitzer, *Fermi Surfaces of Low-Dimensional Organic Metals and Superconductors*, Springer-Verlag, Berlin, 1996.
- [19] C. E. Campos, P. Sandhu, J. S. Brooks and T. Ziman, *Phys. Rev. B* **53** (1996) 12725.
- [20] J. Schmalian, *Phys. Rev. Lett.* **81**, 4232(1998).
- [21] X. Su, F. Zuo, J. A. Schlueter, J. M. Williams, P. G. Nixon, R. W. Winter and G. L. Gard, *Phys. Rev. B* **59** (1999) 4376.
- [22] F. Zuo, J. A. Schlueter and J. M. Williams *Phys. Rev. B* **60** (1999) 574 and references therein.
- [23] C. H. Mielke, N. Harrison, D. G. Rickel, A. H. Lacerda, R. M. Vestal, L. K. Montgomery, *Phys. Rev. B* **56** (1997) R4309.
- [24] K. Maki, E. Puchkaryov, H. Won, *Synth. Met.* **103**, 1933(1999).
- [25] M.V. Kartsovnik, G. Yu. Logvenov, K. Maki, and N.D. Kushch, *Synth. Met.* **103**, 1827(1999).
- [26] M. Maesato, Y. Kaga, R. Kondo, S. Kagoshima, *Rev. Sci. Instrum.*, to be published (1999).
- [27] K. Murata et al., to be published.
- [28] H. Kusunohara, Y. Sakata, Y. Ueba, K. Tada and M. Kaji, *Solid Stat. Commun.* **74** (1990) 251.
- [29] M. Kund, J. Lehrke, W. Biberacher, A. Lerf and K. Andres, *Synth. Met.* **70** (1995) 949.
- [30] M. Lang, R. Modler, F. Steglich, N. Toyota and T. Sasaki, *Physica B* **194-196** (1994) 2005.
- [31] J. Caulfield, W. Lubczynski, F. L. Pratt, J. Singleton, D. Y. K. Ko, W. Hayes, M. Kurmoo and P. Day, *J. Phys.: Condens. Matter* **6** (1994) 2911.

Uniaxial and Hydrostatic Pressure Dependence of T_c for $\kappa(\text{ET})_2\text{Cu}(\text{NCS})_2$: $\Delta T_c/\Delta P$ (K/kbar)			
	a -axis	b -axis	c -axis
Uniaxial (This work samples 1,2 4, and 5)	-0.78	0+ < 3 kbar -0.2 < 3 kbar	-0.2
Uniaxial (This work-sample 3)	-	+0.3 < 2 kbar -0.08 > 2 kbar	
Uniaxial[16]	-2	-	-
Tensile stress (ΔT_c) [28]	-	+0.5 ~ 0.8K	-
Thermal expansion (Kund)[29]	-3.2	0.0	+1.46
Thermal expansion (Lang)[30]	-6.2	-0.14	+3.44
Hydrostatic[31]	-3		

Table 1

Summary of the effects of uniaxial and hydrostatic pressure on the superconducting transition temperature T_c of κ -(BEDT-TTF) $_2$ Cu(SCN) $_2$.

Uniaxial and Hydrostatic Pressure Dependence of SdH Frequencies: κ -(BEDT-TTF) $_2$ Cu(SCN) $_2$: $\Delta F/F_0/\Delta P$ (% kbar)		
Uniaxial (this work)	F_α	F_β
a -axis	+3.0[16], 5.0	-0.7
b -axis	-0.25	+0.1
Hydrostatic[31]	+1.84	+0.36

Table 2

Summary of the effects of uniaxial and hydrostatic pressure on the Fermi Surface topology of κ -(BEDT-TTF) $_2$ Cu(SCN) $_2$.

Fig. 1. a) Molecular stacking (the oval structure indicates each BEDT-TTF molecule) and the equivalent triangular lattice with transfer integrals t_1 and t_2 . b) The Fermi surface of κ -(BEDT-TTF) $_2$ Cu(SCN) $_2$ at ambient pressure. The fundamental α and breakdown β orbits are also shown.

Fig. 2. Resistance vs. temperature as a function of applied uniaxial stress along the c-axis for Sample 1. Inset: T_c values are obtained from gaussian fits to the peaks in the derivative dR/dT .

Fig. 3. Summary of resistance vs. temperature data for 0, 2.5, and 5 kbar for all uniaxial stress directions.

Fig. 4. Summary of the uniaxial stress dependence of the superconducting transition T_c for all stress directions studied.

Fig. 5. Magnetoresistance of sample 5 at 0.5 K for different values of uniaxial stress along the a-axis.

Fig. 6. a) Fourier spectrum of sample 5 at 0.5 K for different values of uniaxial stress along the a-axis. b) a-axis stress dependence of the β orbit and its difference frequencies. c) a-axis stress dependence of the α orbit. Above 1 kbar, F_α was determined from the difference frequencies in b).

Fig. 7. Critical field B_{c2} of sample 5 at 0.5 K vs. a-axis stress. Inset: The peaks in the derivatives dR/dB were used to determine the B_{c2} values.

Fig. 8. Magnetoresistance of sample 4 at 0.5 K for different values of uniaxial stress along the b-axis.

Fig. 9. a) Fourier spectrum of sample 4 at 0.5 K for different values of uniaxial stress along the b-axis. b) Shift of the α orbit SdH waveform with b-axis stress. c) b-axis stress dependence of the α orbit derived from b).

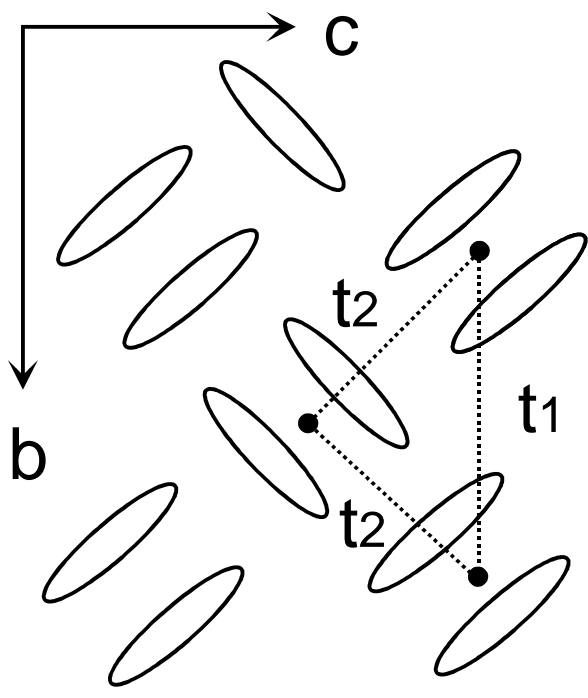
Fig. 10. Critical field B_{c2} of sample 4 at 0.5 K vs. b-axis stress. Inset: The peaks in the derivatives dR/dB were used to determine the B_{c2} values.

Fig. 11. a) Resistive anomaly at 2.0 K in the MR of sample 5 for stress applied along a -axis. b) Resistive anomaly at 2.0 K in the MR of sample 4 for stress applied along b -axis. Note that the resistive anomaly is defined as the difference ΔR divided by the extrapolated normal state resistance R_N shown as the dashed line. A similar construction was used to determine $\Delta R/R_N$ for all data shown.

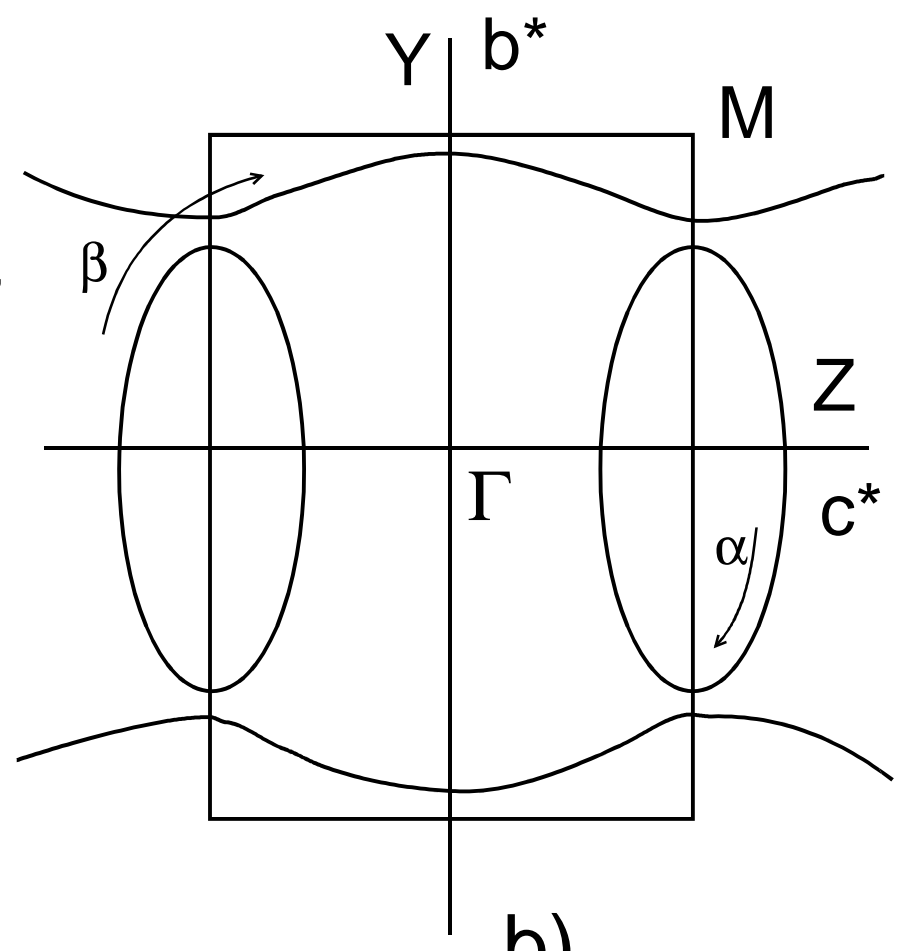
Fig. 12. a) Resistive anomaly $\Delta R/R_N$ for a -axis stress at different temperatures. $\Delta R/R_N$ for b -axis stress at different temperatures.

Fig. 13. Normal state (fractional) resistance change vs. applied stress for samples 4 and 5 (at 26 T and 0.5 K) and for samples 1 and 2 (at 0 T and 14 K). The solid lines are fits to the $1 - (P/10.7)^2$ (sample 4) and $(1 + 0.34P)^{-1}$ (sample 2 and 5), where P is given in kbar.

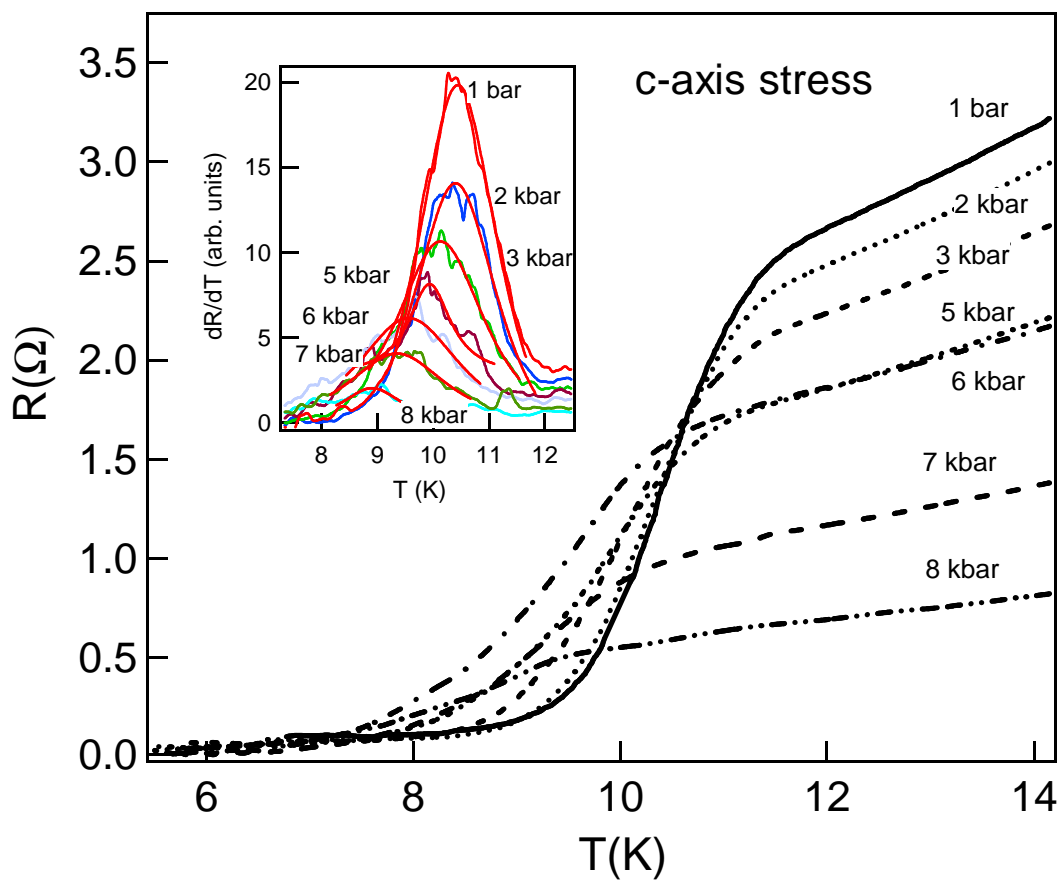
Fig. 14. Effective masses for α and β orbits vs. uniaxial stress.



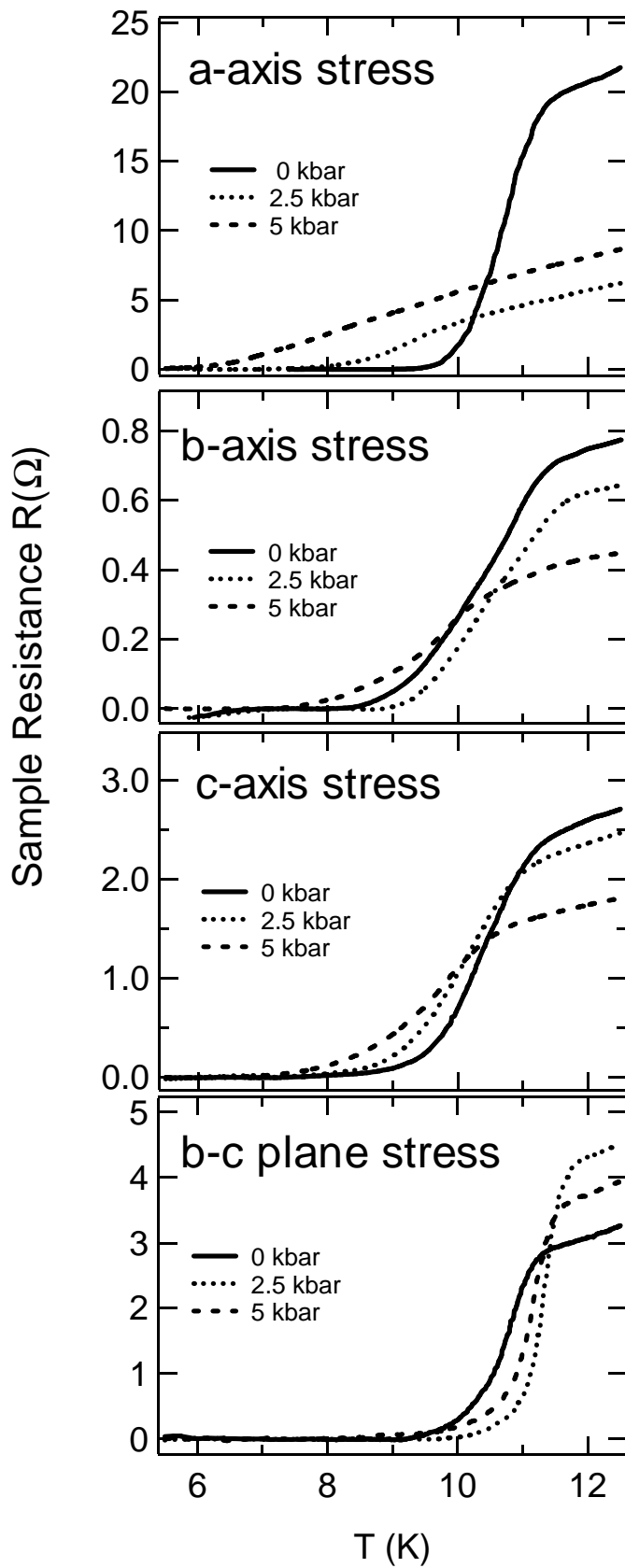
a)



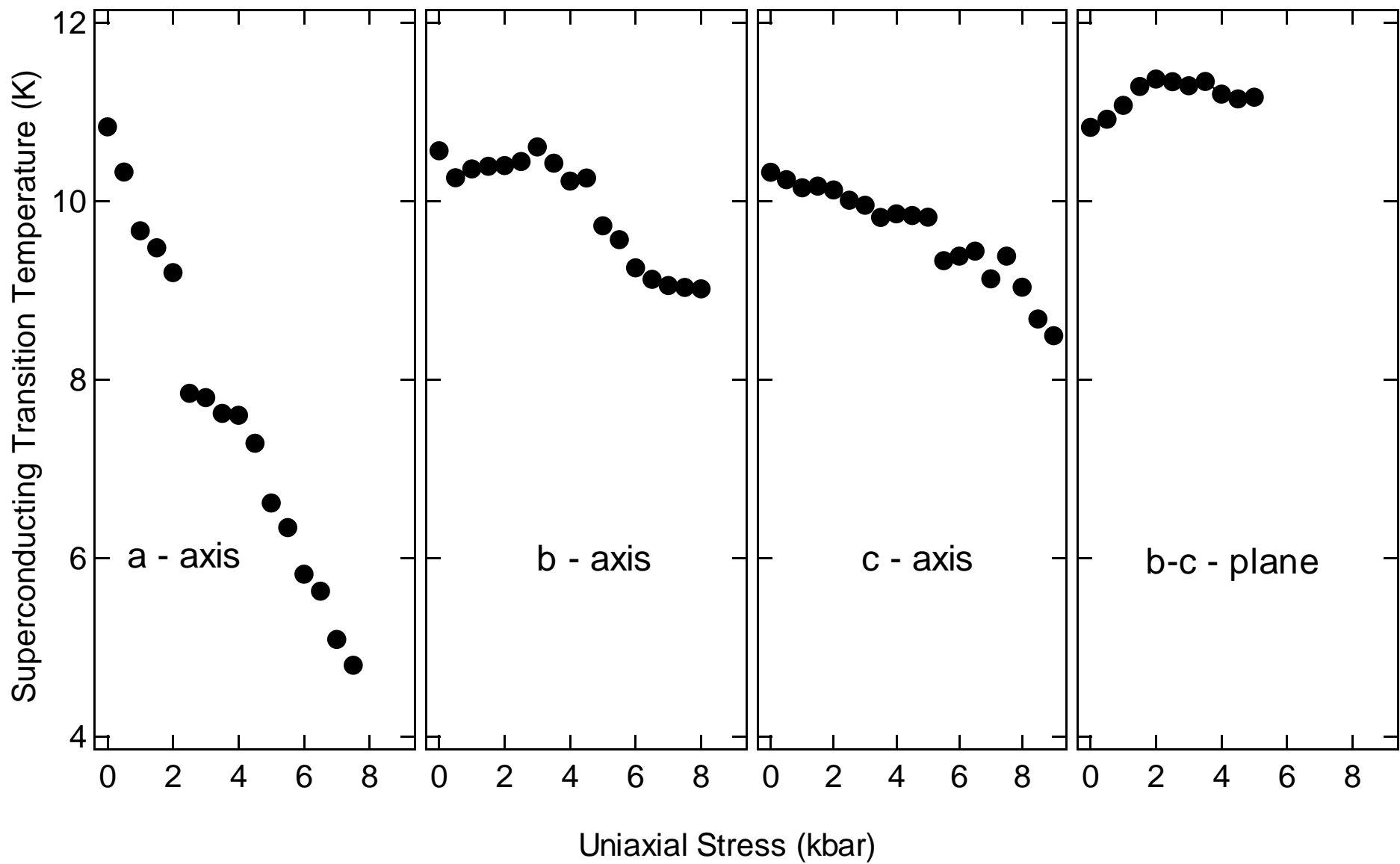
b)

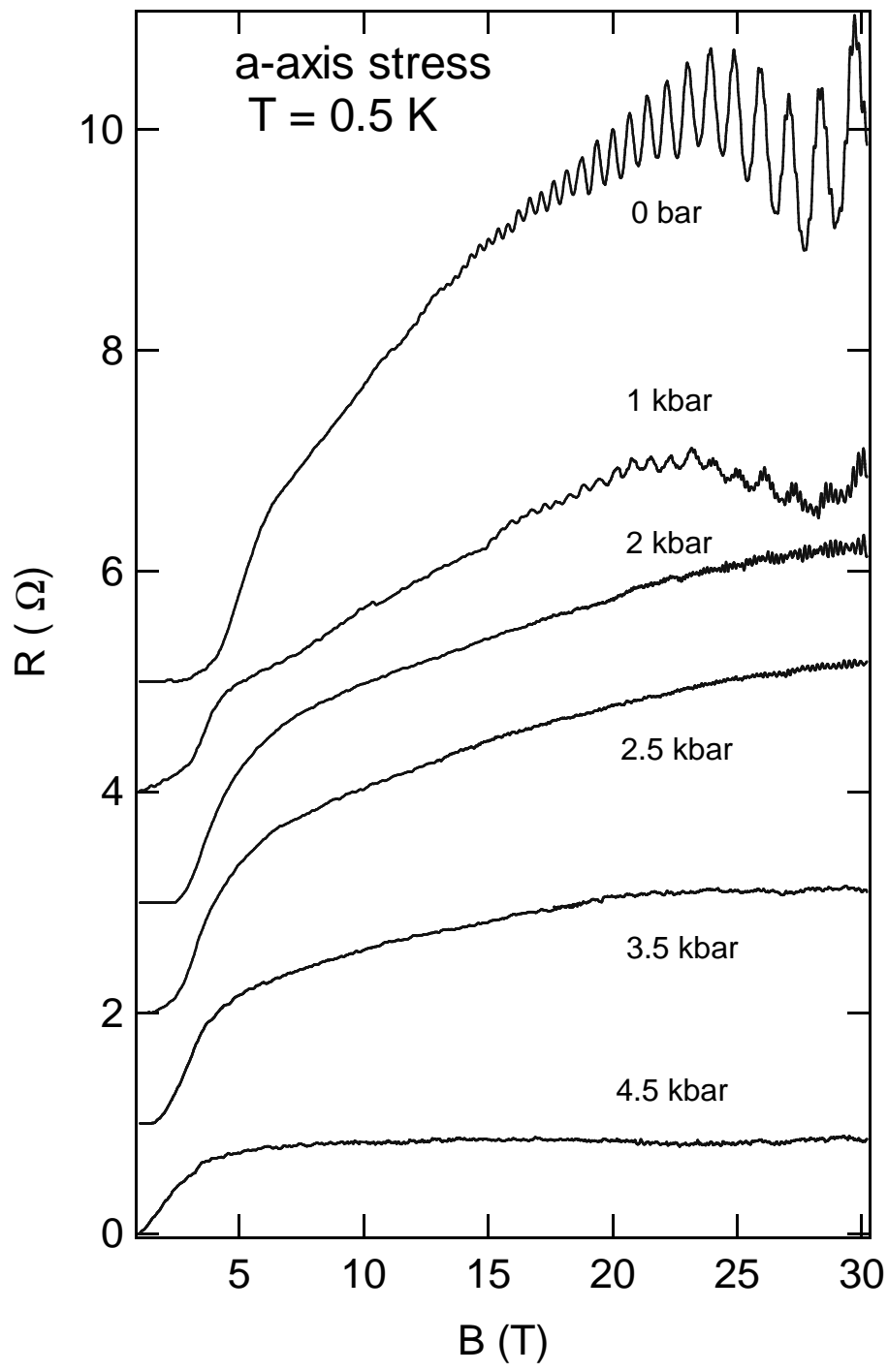


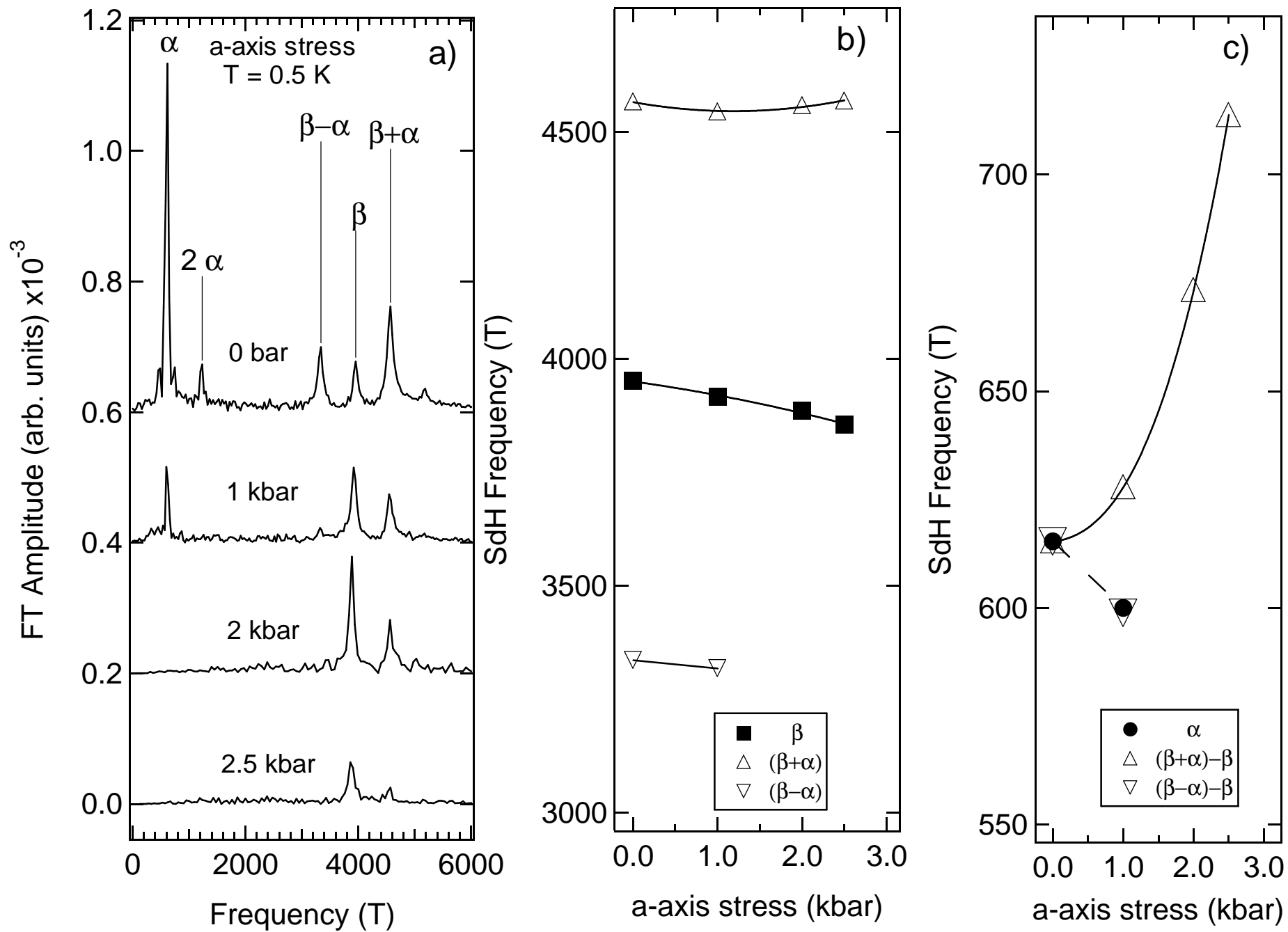
Choi et al., Fig. 2

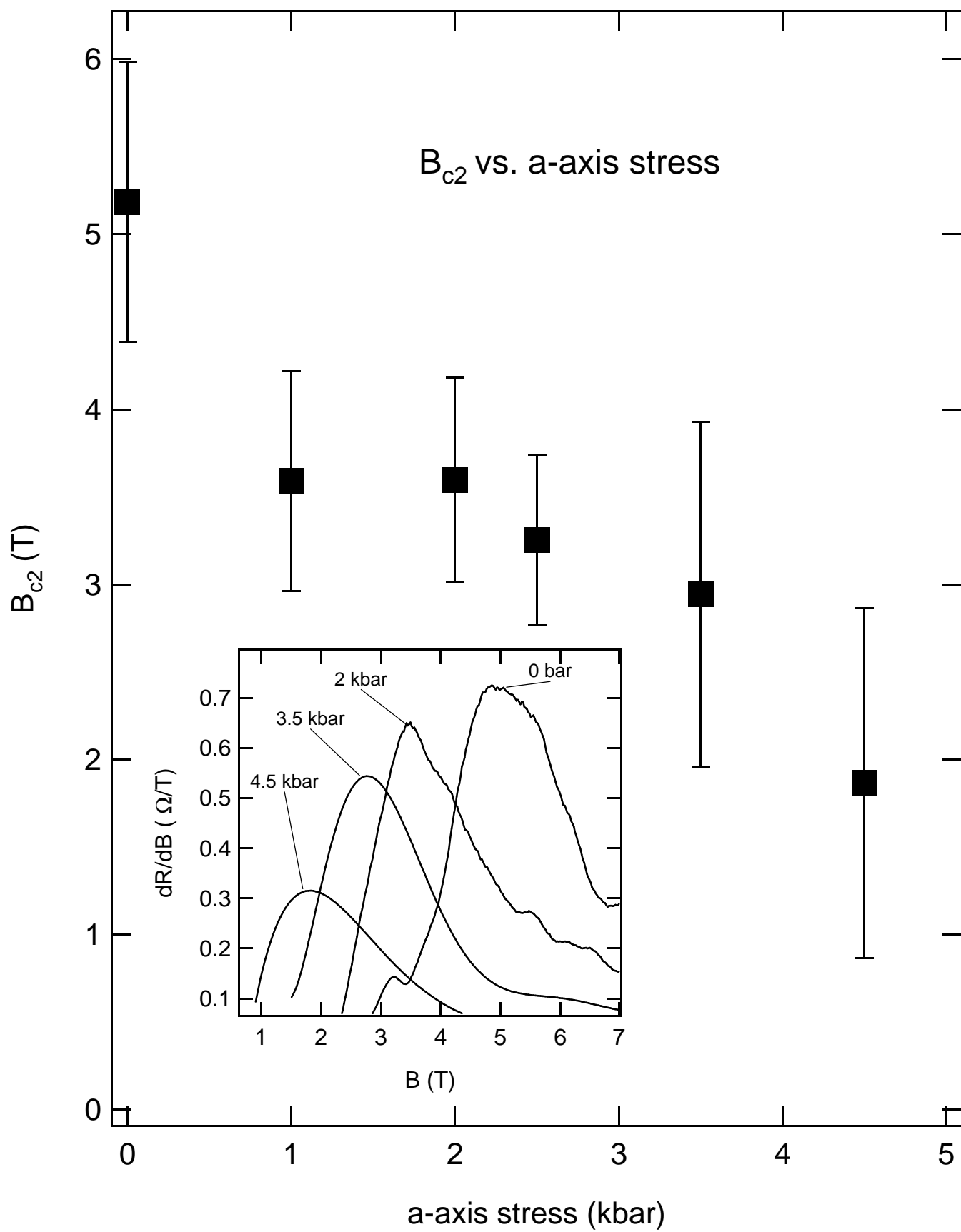


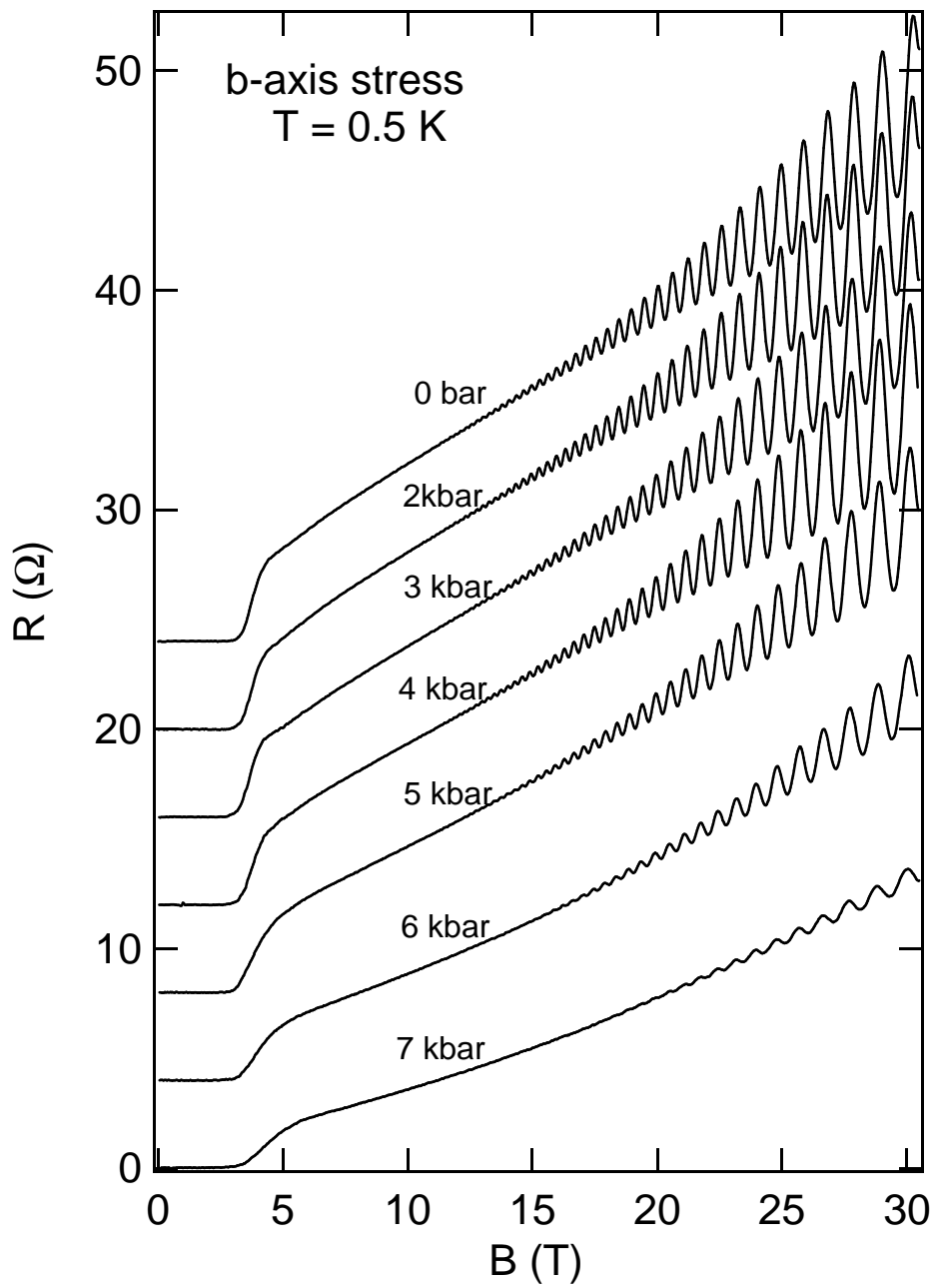
Choi et al, Fig. 3



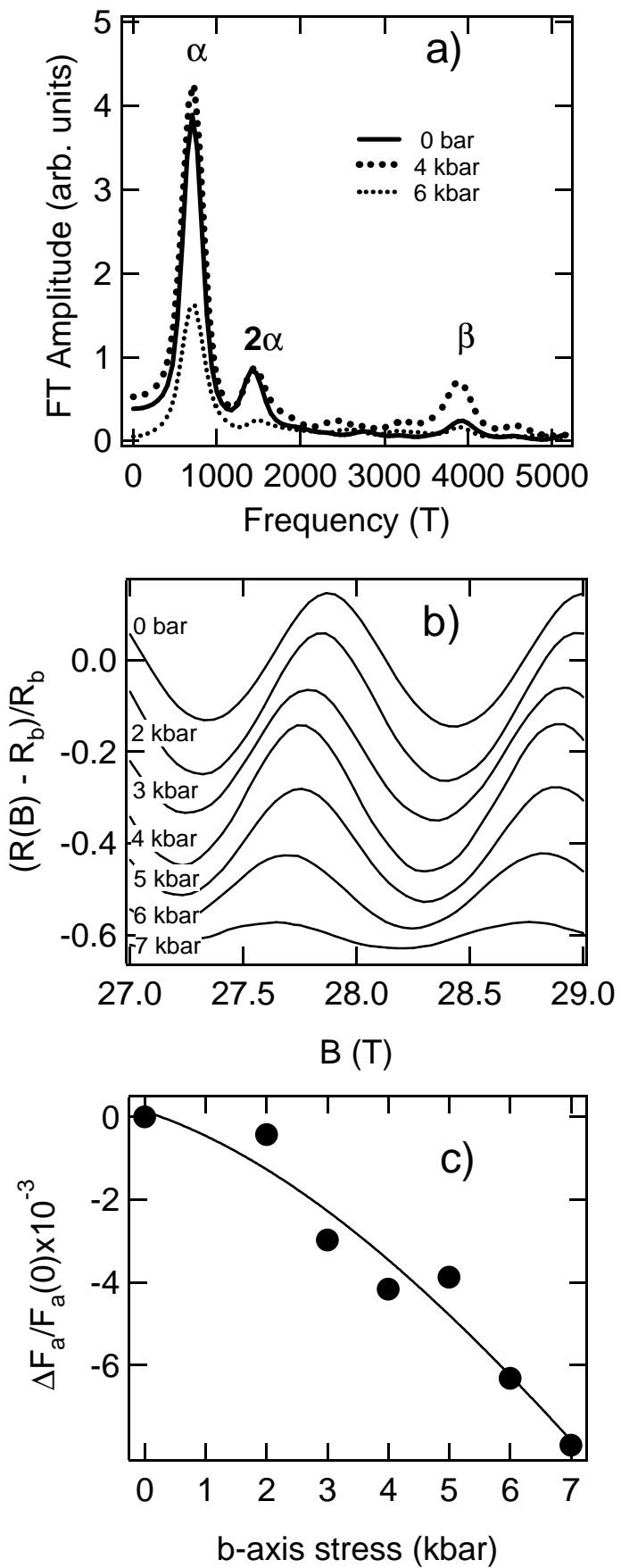


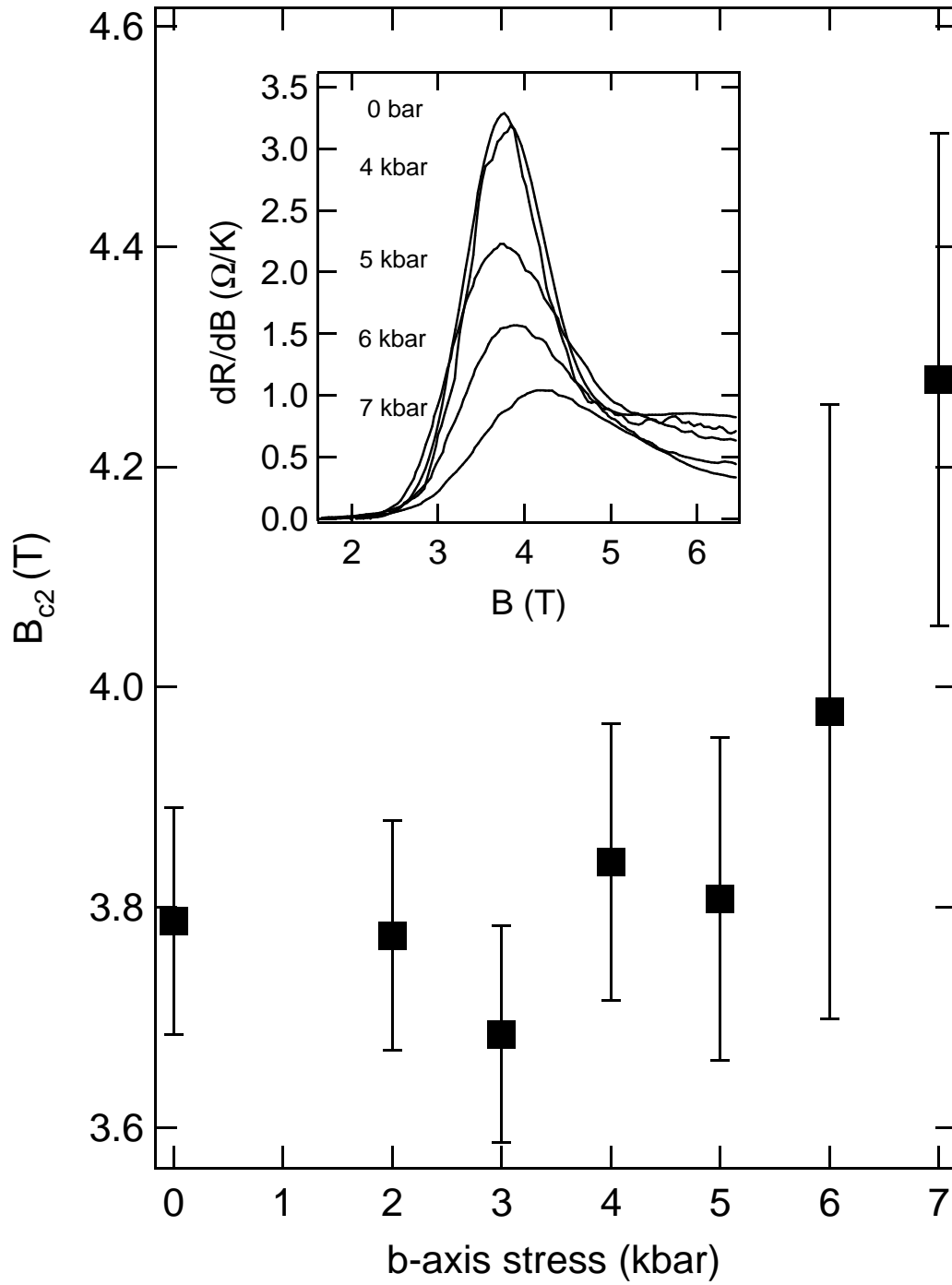


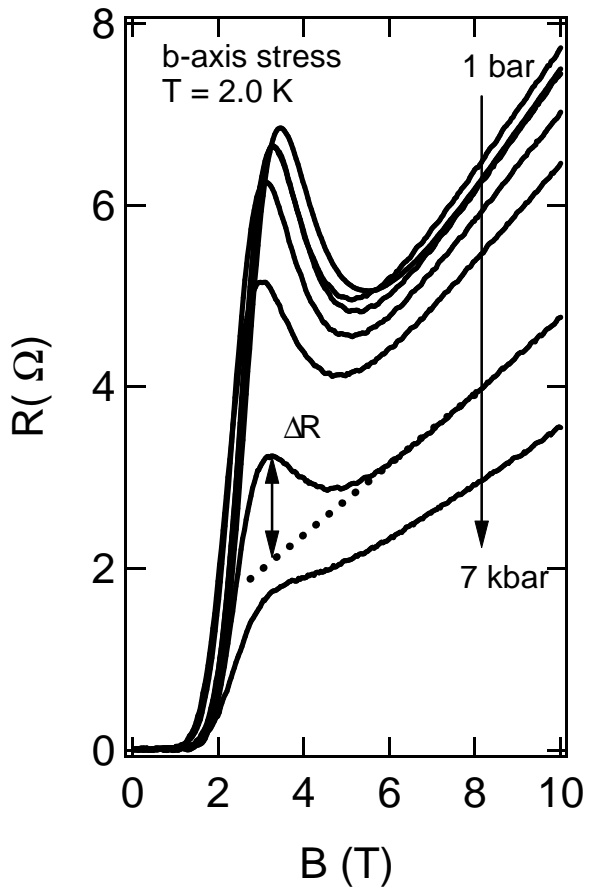
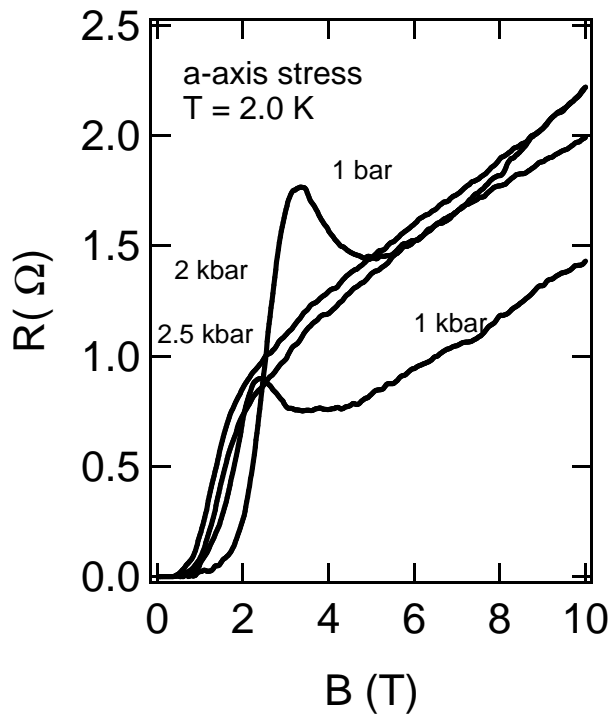


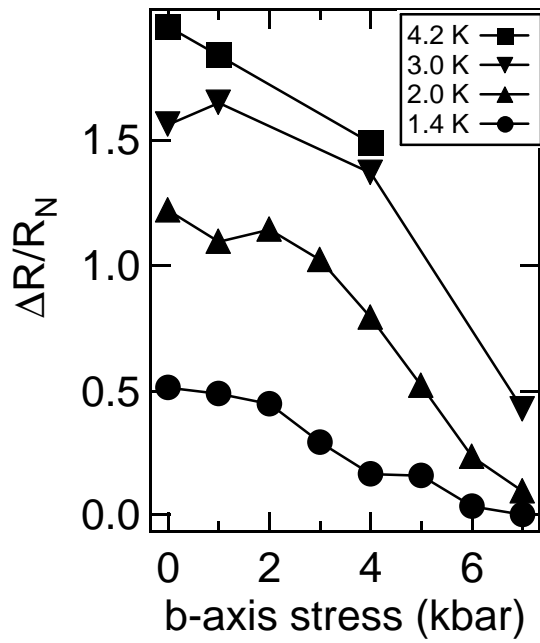
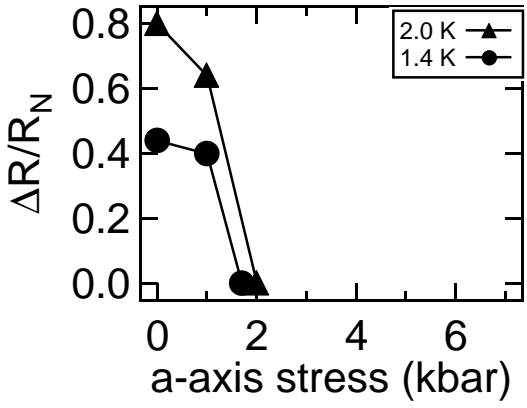


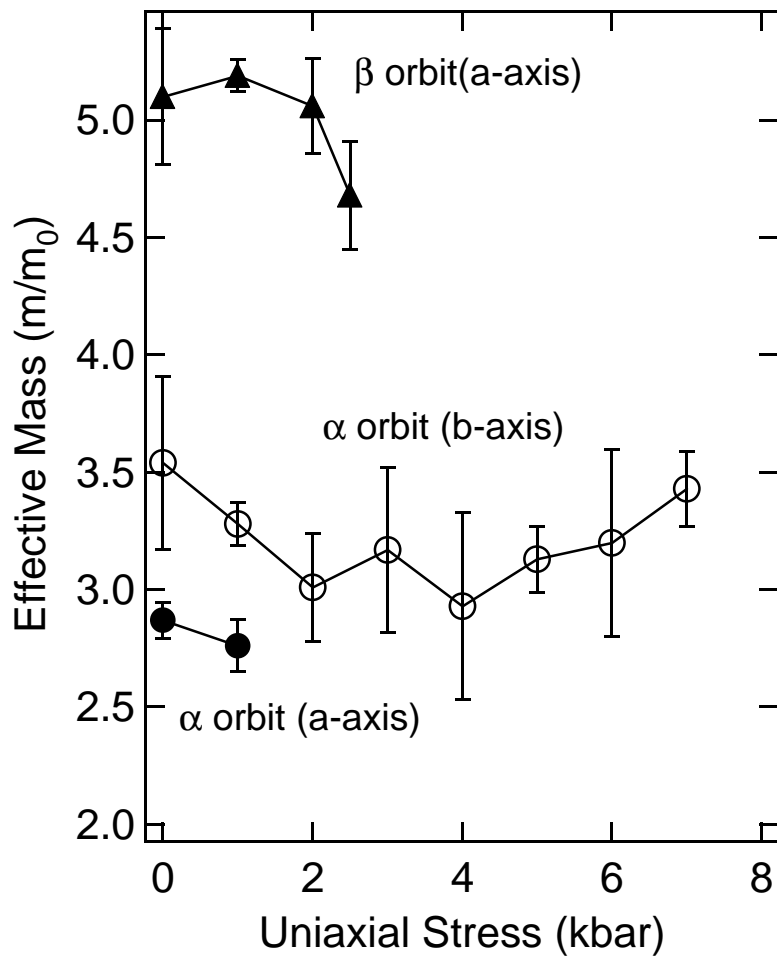
Choi et al., Fig. 8

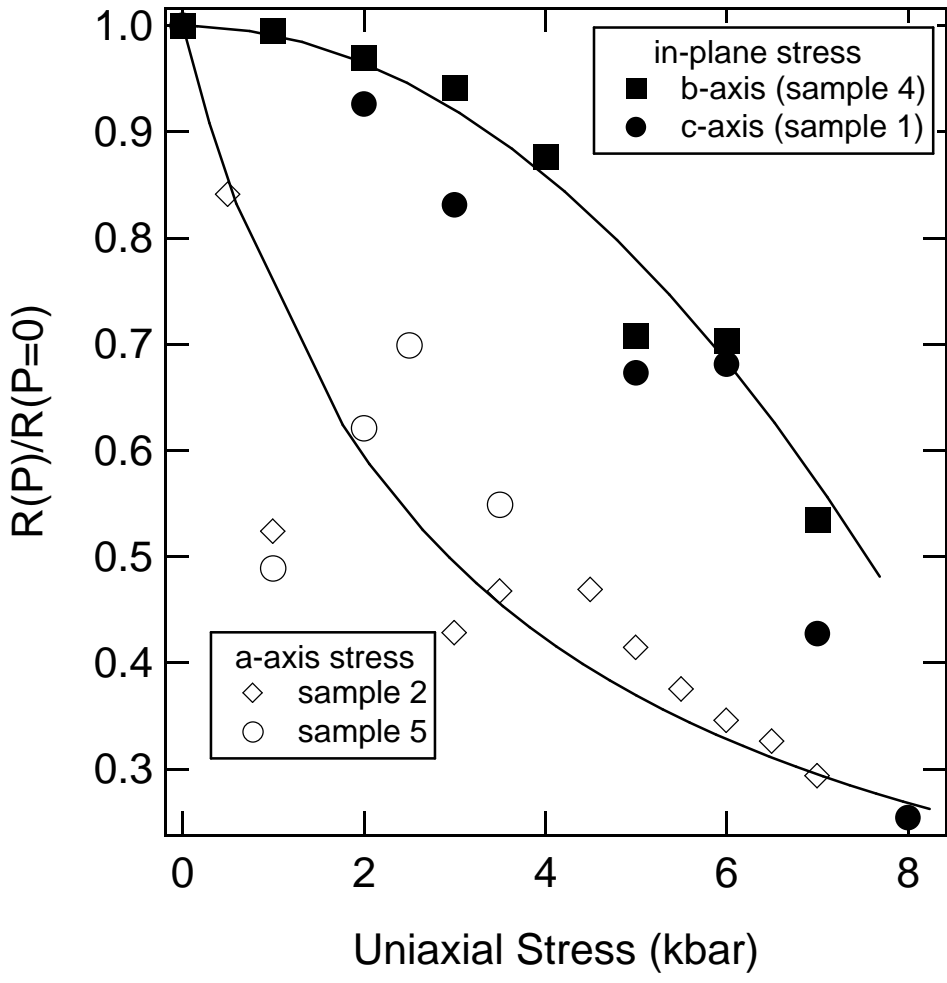












Choi et al., Fig. 14